https://dx.doi.org/10.1016/j.enconman.2022.115600

Developing a novel gasification-based sludge-to-methanol utilization process and exergy-economic-environmental (3E) analysis

Tao SHI[1], Yue LIU[1], Ao YANG[2], Shirui SUN[3], Weifeng SHEN[3], Jingzheng REN[1*]

[1]Department of Industrial and Systems Engineering, The Hong Kong Polytechnic University, Hong Kong SAR, P. R. China.

[2]College of Safety Engineering, Chongqing University of Science & Technology, Chongqing 401331, P. R. China.

[3]Department of Chemistry and Chemical Engineering, Chongqing University, Chongqing 400044, P. R. China.

**Corresponding Author: ***E-mail: jzhren@polyu.edu.hk

Abstract

Sewage sludge is a common waste from wastewater treatment plants in Hong Kong and conventional treatment ways like the landfilling method has been gradually abandoned considering the environmental impacts and costly land. Searching for integrating processes to well treat the sludge simultaneously achieve the energy recovery can be a good alternative way. Therefore, process design and simulation of a gasification-based sludge to methanol (STM) production was proposed in this work. It considered major subsections such as gasification, power generation, absorption, methanol synthesis, and distillation. Followed by the sensitivity analysis to optimize operational parameters, economic, environmental, and exergy (3E) analysis of STM process was conducted. The economic estimation revealed the methanol production cost is 579.62$/ton and the sludge disposal cost is 39.58$/ton. The calculated internal rate of return (IRR) of the process is 10.20% and 5.48%, respectively with a subsidy of 20$/ton sludge and without any support. Moreover, it was found the greenhouse gas (GHG) emission was 3.21 kg eq.CO2/kg methanol and overall exergy efficiency was 57.31%. The current work implies the great potential of STM treatment strategy, which can serve as a reference for the future sludge treatment planning.

Keywords: Sludge gasification, Waste to energy, Exergy analysis, GHG emission, Internal rate of return

1. Introduction

Huge amount of wastewater in modern city has raised a growing attention on the study of its sustainable treatment [1]. Sewage sludge is a residue solid-liquid mixture that generated from such wastewater treatment processes. It contains a high proportion of moisture and thereby the volume is large. The direct objectives of sludge treatment are to reduce the volume and to stabilize the material by destructing some pathogenic microorganisms [2]. In the case of Hong Kong, it receives about 380 kilo tons of sewage sludge per year from 11 collection centers [3]. For the goal of sustainable development of Hong Kong, exploration and valorization of sewage sludge is necessary. Liu et al [4] has reviewed the developments of utilizing sludge to produce hydrogen and compared the specified technologies in terms of their advantages and drawbacks. From the review, biological conversion has the cost superiority however it cannot substantially reduce the sludge volume. On the other hand, gasification method has the superiority in technical readiness level and pollution alleviation among thermochemical processes, it has been widely studied before with the expectation of achieving the circular economy [5]. Gasification technology can convert waste resources into a syngas mixture containing carbon monoxide (CO), hydrogen (H_2), carbon dioxide (CO_2), vapor water, methane (CH_4) and other light combustible hydrocarbons (C_xH_y) which could serve as precursors to produce waste-based fuels or value-added chemicals [6, 7]. Owing to the complex mechanism of the gasification, some experimental investigations have been carried out to contribute more on the kinetics of syngas production [8, 9] or the feedstock decomposition [10, 11]. Followed by the laboratory results, conceptual design by process simulation can be applied as a representative scale up way to explore the real conditions during the establishment of gasification plants [12]. For example, Hantoko et al [13] investigated the supercritical water gasification (SCWG) of sewage sludge for hydrogen production by using a thermodynamic equilibrium model, in which various operation factors were analyzed in detail. Zhang et al [14] reported an enhanced SCWG integrated system for sludge treatment and the thermodynamic analysis was conducted accordingly using sensitivity analysis. Different from the gasification simulation using Aspen Plus platform, another suitable mathematical model considering the thermodynamic equilibrium was formed in Matlab platform by Bijesh et al [15]. They explored the effects of temperature and equivalence ratio on the molar distribution of gas products. Notably, Yang et al [16] established a commercial biomass intermediate pyrolysis poly-generation process using

Aspen simulation tool and shows the prospective contribution of biomass utilization to China's carbon reduction goal. Although the literatures made some contribution on the gasification model and operational conditions, limited work on the utilization of the sewage sludge in Hong Kong has been analyzed so far. Whether the gasification treatment of sewage sludge can be economically feasible for future policy making in Hong Kong is worth to be studied.

One of the downstream products of gasification syngas was methanol, which has been seen as a promising fuel and essential chemical raw material which can be used to produce olefins, acetic acid, formaldehyde, and methyl tertiary butyl ether (MTBE) in the chemical industry [17]. Generally, two different pathways for the methanol production are biological and thermochemical process, in which thermochemical conversion using primary energy resources like natural gas (NG) as the raw material to achieve the methane reforming was mainly applied currently [18]. However, considering the huge carbon emission in conventional production and nonrenewable nature of coal and NG, developing alternative processes to achieve the methanol production from other feedstocks is a promising approach. For example, Hernández et al [19] make an optimization of the biogas-to-methanol synthesis process based on mathematical models. Optimization results with the environmental and economic objectives shown the biogas composition should be around 50% CH_4 and 47% CO_2. Similarly, Santos et al [20] established mathematical model of the biogas-to methanol synthesis process and comparably studied various biogas sources namely landfill, palm oil effluent, corn cobs and sorghum formation with the maximum methanol amount. The above investigations did not study the biomass-to-biogas conversion and the major focus was the optimization of biogas-to-methanol synthesis. In regard of this, Puig-Gamero et al [21] proposed the thermochemical conversion process of methanol production by integrating pine gasification, syngas cleaning and methanol synthesis sections. It conducted the analysis of the effects of different variables on the final syngas composition.

As the gasification modelling gets deeper, exergy, economic and environmental (3E) analysis of the systematic process of methanol production from waste or biomass has been gradually investigated, which aimed at validating the technology prospect of waste valorization. For instance, Im-orb et al [22] carried out a thermodynamic analysis of bio-methanol production from oil palm residues using a process model developed in Aspen Plus and it was found the maximum energy and exergy efficiencies were 38.57 and 25.44%, respectively. Moreover, the thermodynamic analysis were extended in the waste valorization processes to produce synthetic fuel [23], power [24] and ethylene glycol [25]. On

the other hand, economic and environmental analysis of such waste valorization has attracted more attention. For example, Menin et al [26] have modelled two biomass gasification-based processes namely the standalone bio-methanation of syngas (SAB) and the integrated biomethane and bio-methanol (IBB) production. Qi et al [27] made a conceptual design of novel municipal sludge-to-hydrogen fuel production based on plasma gasification, in which they analyzed the technical, economic and environmental performance and the economic results has shown a huge potential of sludge-to-hydrogen in sludge treatment. Alves et al [28] finished the development of a techno-economic analysis for a small-scale gasification plant for the production of hydrogen or electricity power. In terms of obtaining the bio-char products, Medina-Martos et al [29] comparably studied the sludge hydrothermal carbonization process however the economic cost was found to be 42% higher than that of standard lone anaerobic digestion. The techno-socio-economic analysis of the sludge-to-biooil pyrolysis conversion was conducted systematically by Shahbeig et al [30]. More recently, a comprehensive analysis was finished for the bio-methanol production from palm wastes steam gasification which applied the carbon capture technology [31]. the calculated profit was around 193.5$/tonne based on the assumption of methanol selling price 430$/tonne and carbon reduction was around 57.25 tonnes CO_2 -e/h. From the literature review, although economic and environmental evaluation on the sludge-to-hydrogen, sludge-to-biooil, sludge-to-biochar, and biomass-to-methanol has been studied, few research have focused on a systematical simulation and the comprehensive analysis from economic, environmental and exergy aspects of sludge-to-methanol (STM) process.

Therefore, according to the requirement of sludge treatment in Hong Kong, this work intend to investigate the gasification-based valorization method to obtain methanol production from waste sewage sludge. The main contributions of this study are: 1) a systematic process from raw sludge to methanol conversion was proposed which involves the gasification treatment and downstream methanol production, 2) the key operational parameters of the STM process were optimized sequentially based on the rigorous simulation by Aspen Plus, and 3) comprehensive analysis were conducted from 3E aspects to provide some suggestions and implications. Specifically, the integrated STM process was mainly comprised of gasification, power generation, absorption, methanol synthesis, and distillation. The gasification model was established through the restrict thermodynamic equilibrium of typical gasification reactions and the adjustment of temperature approach. Then, gasification gases distribution in simulation was compared with that in literatures to make a validation

of the gasification model. Followed by that, the sensitivity analysis was finished to investigate the influence of key factors on the syngas yield and composition. According to the systematic built-up process after optimization, the economic estimation has shown the feasibility of sludge gasification in Hong Kong despite of some subsidy. We also carried out the life cycle GHG emissions to evaluate the environmental impacts. A detailed exergy flow calculation was carried out to identify the energy bottleneck and provide guidelines for further process improvement.

2. Methodology

2.1 Process simulation

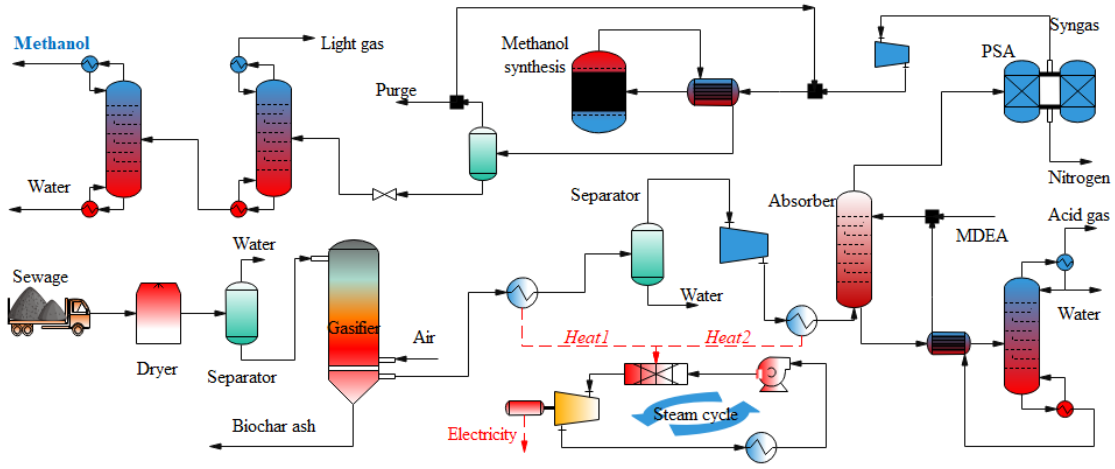

Fig.1 Systematic gasification utilization process of sewage sludge for methanol production

The simplified process flowsheet was shown in **Fig. 1**. It is assumed that the proposed process is a conceptual design and is the major sections of a real-world waste-to-energy plant. Additional pips and valves were not displayed in the process flowsheet. Five major operation units were involved such as the air gasification, steam-cycle power generation, gas removal, methanol synthesis and methanol distillation separation. The sewage sludge was generated during treatment of wastewater from different sites in Hong Kong. After collecting the sewage sludge in a centralized disposal site, the sludge was dried under the atmosphere of high-temperature steam. Most of the bacteria and virus would be killed and then moisture be removed to adjust the water flowrate into the gasifier. Gas mixture emitted from the downdraft gasifier was a heat source that can evaporate the high-pressure water into steam and achieve power generation. This integrated process can reduce the electricity consumption in other operations. Flue gas contained H_2S gas which is highly toxic and can deactivate catalysts in the methanol synthesis. Therefore, acid gas must be absorbed and stored to avoid the damage. Then inert

nitrogen gas can be separated through pressure swing adsorption (PSA) technology. Nitrogen gas is popular and valuable product in the gas market. Through the gas cleaning section, purified syngas with main components CO, H_2, CH_4, CO_2 and H_2O were sent into the synthesis reactor to synthesize methanol. Eventually, distillation process achieved the separation of methanol product with 99.9 mol%. Complete process simulation was built up in the Aspen platform with their detailed model specifications, which has been shown in **Fig. A1** and **Table A1**, respectively. Detailed demonstration of each simulation is given in the following subsections.

2.1.1 Gasification process

Similar to the biomass gasification, the complete simulation of waste sludge gasification can be seen as three stages namely drying, pyrolysis and gasification stages. The dryer was modelled using a Rstoich reactor block which can convert a part of nonconventional sludge into water according to the conversion reaction (see **Eq. (1)**).

$$Sludge \rightarrow 0.0555084 H_2O \quad (1)$$

Since the feedstock of sewage sludge was introduced in Aspen Plus as a nonconventional component, before going into the gasification reactor, it should be decomposed into its elements namely the conventional components. Therefore, another RYield reactor unit was applied to simulate the pyrolysis process according to the ultimate analysis of the sewage sludge. This is NOT a true standalone reactor, but an integral part of the gasification reactor which provides the simplicity to determine various species like solid carbon, hydrogen, nitrogen, oxygen, sulphur, bounding water and ash. Then, inert ash was separated by a cyclone separator before they were introduced into the gasification reactor. Based on the experimental research, **Table 1** has shown the industrial analysis composition of sewage sludge in detail.

Table 1. The typical composition of sewage sludge in Hong Kong [32]

Proximate analysis (wt%)		Ultimate analysis (wt%)	
Moisture	64.1	C	47.54
Volatile matter	75.3	H	7.99
Fixed carbon	1.3	O	18.55
Ash	23.4	N	2.02
		S	0.5

A common method was used in this work for gasification modelling by estimating thermodynamic equilibrium through calculation of Gibbs energy minimization. However, real operation cannot reach

the idea equilibrium condition. Therefore, the temperature approach was adjusted to obtain model predictability by restricting some predefined reactions in the Gibbs reactor [33, 34]. In this work, specified outlet components and restricted reactions have been given in **Table 2**. Notably, the number of involved atoms plus that of linearly independent reactions must equal to the total number of products.

Table 2. Specified components and restricted reactions of the gasification Gibbs reactor [33]

Involved atoms	Restricted reactions	Specified output products
C	R1: $C + CO_2 \rightarrow 2CO$	H_2
H	R2: $C + H_2O \rightarrow CO + H_2$	C
O	R3: $CO + H_2O \rightarrow CO_2 + H_2$	CO
N	R4: $CH_4 + H_2O \rightarrow CO + 3H_2$	CO_2
S	R5: $C + O_2 \rightarrow CO_2$	H_2O
		NH_3
		N_2
		H_2S
		CH_4
		O_2

Additionally, some basic assumptions were made to simplify the downdraft gasifier before conducting the simulation [35]: 1) the gasification system is at steady state isothermal condition, 2) the nitrogen and sulphur were fully converted into NH_3 and H_2S, 3) ash is inert and tar formation are neglected because of the low content in the outlet gas stream from downdraft gasifier, 4) char only contains carbon and ash. PR-BM physical model was used in the gasification stage since it can well estimate the properties of such hydrocarbon and light gases in a fairly high temperature condition. Components like ash and the sewage sludge have been set as non-conventional component. Enthalpy and density estimation of non-conventional sludge and ash was finished using HCOALGEN and DCOALGT model. The HCOALGEN model includes several correlations for the heat of combustion, formation, and heat capacity which can be found in the Aspen Help files. In the present work, the setting of HCOALGEN model was 6-1-1-1 which means the heat of combustion is user defined and the heat of combustion of sewage sludge selected in this work is 25.63 MJ/kg based on the experimental result [32]. It is worth noting that gasification is not autothermal and additional fuel must be supplied to meet the gasification requirements. Through the three steps, a sewage sludge gasification process can be understood by a universal equation (see **Eq. (2)**).

$$\text{Sludge} + \text{gasification agent} \xrightarrow{heat} CO + CO_2 + H_2O + H_2 + NH_3 + H_2S + C_nH_m + C_xH_yO_z + Ash \quad (2)$$

Aromatic tar ($C_xH_yO_z$) components generated during the intermediate low-temperature pyrolysis was ignored since downdraft gasification is recognized to produce insignificant such contents [36]. Independent gasification reactions that considered were listed in **Table A2** in the **Appendix. A** [37]. The downdraft gasifier was operated in the atmospheric pressure and the temperature of dryer, pyrolysis and gasification were 101, 500 and 800 ℃ [38].

2.1.2 Power generation

As shown in **Fig. 1**, the high-temperature gas from gasifier can be used to vaporize waster and achieve the power generation. This integrated gasification that combined cycle can be found more detail in the studies [39, 40]. Herein, steam cycle was applied owing to the availability of water. It consists of a heat recovery evaporator, steam turbine, pump, and condenser. There are two steam cycle processes for the power generation. The first heat comes from the raw syngas produced from downdraft gasifier. And the second heat exchanger is used to recover the inner energy of compressed syngas followed by connecting an absorption column. To make the power generation process converge, following procedures were conducted. Firstly, a suitable feed flowrate should be found with appropriate heat-exchange conditions where no cross-temperature exists. In detail, a design specification was set to vary the feed flow rate to attain a suitable cold stream outlet temperature in which the outlet steam has been completely vaporized. Then, pressures of discharged stream from pump and turbine were determined through the sensitivity analysis with the aim of maximum power generation. Considering the complete condensation of recycled steam from turbine and the required minimum temperature difference of 5℃ between it and utility water, the discharged pressure of turbine cannot be too small.

2.1.3 Acid gas removal process

The composition of inlet syngas to the absorber column has been given in **Table 3**. It contains undesirable compounds like H_2S and NH_3 which have harmful effects on the downstream methanol. Therefore, this section aims to separate those acid gas and the remaining gas can be introduced into the methanol synthesis reactor. The process described in this work has shown a typical absorption system. More detailed information about the simulation of the amine solvent absorption can be found in the tutorial book [41]. In this work, absorption model was built up on the chemical reactions basis with a methyl diethanolamine (MDEA) solution. MDEA as a tertiary ethanolamine was selected due to its higher selectivity absorption of H_2S compared to other amine solvents [42]. Another advantage

of using MDEA is the lower heat of regeneration process than other amines, which is helpful in reducing the total energy consumption of the desorption column.

Table 3 The composition of raw syngas that flow into the absorption column

Composition	Mole flowrate (Kmol/h)	Mole fractions
H_2	1109.8203	0.5264
CH_4	2.6474	0.0013
CO	441.0581	0.2092
CO_2	200.8162	0.0953
H_2O	5.6913	0.0027
N_2	345.0911	0.1637
NH_3	0.6240	0.0003
H_2S	2.5377	0.0012

Contact between the amine solvent and raw syngas causes the chemical reactions and produces the absorption effects. Both kinetic reactions and equilibrium reactions were adopted in the absorber column. In this study, the associated chemical reactions include the CO_2-MDEA-H_2O, H_2S-MDEA-H_2O and NH_3-CO_2-H_2O systems when syngas are dissolved in MDEA solution. Reactions between H_2S and MDEA are primarily faster than CO_2 and MDEA owning to the selectivity of MDEA. The governing equilibrium ion reactions with detailed equilibrium constant were given in **Table 4**. It should be noted that the reaction equilibrium constant was calculated as a function of temperature which can be shown in the following equation.

$$\ln(K_{eq}) = A + \frac{B}{T} + C\ln T + DT \tag{3}$$

Table 4 Equilibrium reactions with adopted equilibrium constant parameters [42]

Equilibrium reactions	Equilibrium constant			
	A	B	C	D
$2H_2O \rightleftharpoons H_3O^+ + OH^-$	132.90	-13445.90	-22.48	0
$H_2O + NH_3 \rightleftharpoons NH_4^+ + OH^-$	-1.26	-3335.70	1.50	-0.04
$H_3O^+ + MDEA \rightleftharpoons MDEAH^+ + H_2O$	-9.42	-4234.98	0	0
$H_2O + H_2S \rightleftharpoons HS^- + H_3O^+$	214.58	-12995.40	-33.55	0
$H_2O + HS^- \rightleftharpoons H_3O^+ + S^{2-}$	-9.74	-8585.47	0	0
$H_2O + HCO_3^- \rightleftharpoons CO_3^{2-} + H_3O^+$	216.05	-12431.70	-35.48	0

On the other hand, absorption of such gases in the solution involves finite rate-controlled reaction while equilibrium cannot be readily attained. Thus, some kinetic-controlled reactions have to be introduced for the description of the absorption phenomenon. **Table 5** has given the chemical reactions associated with detailed kinetic parameters and the rate law equation of kinetic reactions can be presented by **Eq. (4)**.

$$K = k_0 \bullet \left(\frac{-E_a}{RT} \right) \quad (4)$$

Table 5. Kinetic parameters for rate-law reactions [42]

Kinetic reactions	Equilibrium constant	
	k_0	E_a (KJ/mol)
$CO_2 + OH^- \rightarrow HCO_3^-$	4.32e+13	55.47
$HCO_3^- \rightarrow CO_2 + OH^-$	2.38e+17	123.31
$MDEA + CO_2 + H_2O \rightarrow MDEA^+ + HCO_3^-$	2.19e+06	31.10
$MDEA^+ + HCO_3^- \rightarrow MDEA + CO_2 + H_2O$	8.89e+11	64.30
$NH_3 + CO_2 + H_2O \rightarrow NH_2COO^- + H_3O^+$	1.35e+11	48.50
$NH_2COO^- + H_3O^+ \rightarrow NH_3 + CO_2 + H_2O$	4.75e+20	69.20

Radfrac non-equilibrium separation was adopted as a representative model during the absorber simulation. However, using mass and heat transfer correlations instead of the equilibrium model to predict column performance may suffer from the converge problem. In this work, consistently changing the initial values of a tear stream to reduce the converge error helps to solve the problem. Absorber to "Yes" setting and good temperature estimates should be selected and given when nonconvergent problems exist. Furthermore, the "Broyden" solver was used here for tear convergence. For the chemical absorption process, thermodynamic model ELENRTL was selected in the description of an electrolyte system. Henry components were set according to the wizard of ELENRTL choice, which included H_2, CH_4, CO, CO_2, N_2, NH_3 and H_2S. After separating much of the H_2S from the raw syngas, rich amine solution was further introduced to the regeneration column to recycle the MDEA solvent and obtain the acid gas. For the regeneration of acid gas from the liquid in the form of ion, high temperature with low pressure favours the process. It should be noted that the regeneration temperature cannot exceed the amine degradation condition approximately 137 ℃ [43]. For the regeneration column, only vapor-liquid equilibrium parameter was applied as the governing consideration as such kinetic reactions are not involved.

2.1.4 Methanol synthesis

After the acid gas removal unit, a synthesis gas exited from the top of the absorber column with a mole fraction lower than 5 ppm H_2S was ready for production of methanol [44]. Following the previous improved process design [45], an acceptable temperature of 240 ℃ and pressure of 75 atm was applied to the methanol synthesis. The purified syngas was first pressurized and heated before being introduced into the reactor. Then, a purge stream is used to prevent the buildup of inert gases in the reactor and control the amount of recycle stream. Detailed chemical reactions using the commercial

catalyst $Cu/ZnO/Al_2O_3$ was shown in **Table 6**. The particle density and fixed bed voidage of the applied catalyst were 1935kg/m3 and 0.38, respectively.

Table 6. Methanol synthesis reactions on the $Cu/ZnO/Al_2O_3$ catalyst [45]

Kinetic reactions	Reactions	Molar reaction enthalpy (25℃)
CO_2 hydrogenation (R1)	$CO_2 + 3H_2 \rightleftharpoons CH_3OH + H_2O$	-49 kJ/mol
Reverse water gas shift (R2)	$CO_2 + H_2 \rightleftharpoons CO + H_2O$	+41 kJ/mol
CO hydrogenation (R3)	$CO + 2H_2 \rightleftharpoons CH_3OH$	-91 kJ/mol

Only two reactions of the methanol synthesis were independent therefore only R1 and R2 are implemented in the simulation tool. Owing to the governing effect of R1 thus total exothermal performance can be seen in the reactor. It can be implied from the reaction information that to produce more methanol, high pressure with low temperature can be favorable. The reaction kinetics on catalyst $Cu/ZnO/Al_2O_3$ have been widely studied. A common accepted kinetic description by Bussche et al [46] was the basis of this simulation (see **Eq. (5)-(6)**). It should be noted that the original parameters should be calculated and adjusted to directly imported into the process simulator.

$$R1: r_{CH3OH} = \frac{k_1 P_{CO_2} P_{H_2} - k_6 P_{H_2O} P_{CH_3OH} / P_{H_2}^{\ 3} P_{CO_2}}{(1 + k_2 P_{H_2O} / P_{H_2} + k_3 P_{H_2}^{\ 0.5} + k_4 P_{H_2O})^3} [\frac{mol}{kg_{cat} s}] \quad (5)$$

$$R2: r_{RWGS} = \frac{k_5 P_{CO_2} - k_7 P_{H_2O} P_{CO} / P_{H_2} P_{CO_2}}{1 + k_2 P_{H_2O} / P_{H_2} + k_3 P_{H_2}^{\ 0.5} + k_4 P_{H_2O}} [\frac{mol}{kg_{cat} s}] \quad (6)$$

$$\ln k_i = A_i + B_i / T \quad (7)$$

The two reactions were in vapor phase expressed in partial pressure (Pa) of involved chemicals. All kinetic constants were described by the transformation of Arrehenius law as shown in **Eq. (7)**. Parameters of the involved kinetic constants were summarized in **Table 7.** A multitube reactor configuration was set in this study according to the study by Luyben [47] with the length and diameter of 12.2 and 0.0375 meter, respectively.

Table 7. Kinetic constants of methanol synthesis reactions on the $Cu/ZnO/Al_2O_3$ catalyst [48].

Kinetic constant	A_i	B_i (J/mol)
k1	-29.87	4811.2
k2	8.147	0
k3	-6.452	2068.4
k4	-34.95	14928.9
k5	4.804	-11797.5
k6	17.55	-2249.8
k7	0.1310	-7023.4

2.1.5 Methanol distillation

Crude methanol contained some unreacted hydrogen, CO_2 and water, which should be further separated to obtain high-purity methanol product. This is the aim of the methanol distillation process. The first distillation column was used to separated most of light gas while the second distillation column was applied to separated water from the methanol-water mixture. Both columns were simulated with rigorous Radfrac model. It is worth noting that by-products like methyl formate and alcohols were not included the methanol synthesis. Thus, azeotropic phenomenon did not exist in the methanol distillation process. Light gas with mainly CO_2 was collected in a partial condenser. Considering an effective utilization of refrigerant (-25 ℃), 20 atm of the top of distillation column was selected. While the other distillation column was operated in 1 atm. Also, deign specification was conducted to obtain the separation task with 99.9% molar recovery and 99.9 molar purity of methanol.

2.2 Economic, environmental and exergy analysis

2.2.1 Economic evaluation

The major economic evaluation in this work is based on the research by Zhang et al [49]. The total plant cost considered in this study is comprised of two major parts namely the capital cost (*CAPC*) and the operating cost (*OPEC*). *CAPC* includes the equipment procurement (*EPC*) and installation cost (*IC*), indirect capital cost (*ICC*), working capital (*WC*) and the land cost (*LC*) for establishing the gasification (See **Eq. (8)**). *OPEC* comprises the cost of transportation cost (*TC*), feedstock cost (*FC*), utility cost (*UC*), operation and maintenance cost (*O&M*), property tax (*PT*), depreciation cost (*DC*) and general expense (*GE*) and the income tax (*IT*) (see **Eq. (9)**).

$$CAPC = EPC + IC + ICC + WC + LC \tag{8}$$

$$OPEC = TC + FC + UC + O\&M + PT + DC + GE + IT \tag{9}$$

Where *IC* is estimated by 55% of the *EPC* [50]. The *ICC* and *LC* is calculated by 123% and 6% of the total *EPC*. The total *EPC* is summed up based on each single equipment cost which is calculated using the cost correlation method as expressed by **Eq. (10)** [49].

$$EPC = \sum_i \left(EPC_{old} \times \left(\frac{cap}{cap_{old}} \right)^n \times \frac{CEPCI}{CEPCI_{old}} \right) \tag{10}$$

Where EPC_{old} is the base equipment cost from the previous research, besides *cap* and cap_{old} are the capacity of the applied equipment now and before. Noting that the inflation is evaluated based on

the proportion between the chemical engineering plant cost index of different year which are donated as *CEPCI* and $CEPCI_{old}$ [51]. The averaged value of scale factor *n* across the whole chemical industry is about 0.6.

The *ICC* includes the cost like the official application, laboratories, supervision, canteen, auxiliary buildings, and others which are not directly to the equipment aspects. The *WC* is estimated by 5% of the summation of *IC* and *LC*. It can be observed from the above equations that *EPC* plays a crucial role in the total cost. The computation of *EPC* is based on a combination method of cost correlations and Aspen Process Economic Analyzer. Specialized equipment like the gasifier is simulated by different modules together. Therefore, it is better to calculate the purchased cost using cost corrections. Other common equipment like distillation column, compressor and heat exchangers can be well estimated by the economic analyzer tool. For the *OPEC* estimation, the *TC* is computed by the multiplication of transportation weight, distance, and the unit cost of transporting sewage sludge. Since there are few references about the unit transporting cost of Hong Kong and gasoline price in Hong Kong is high, three times of average unit transporting cost in Beijing was finally adopted in the estimation namely 0.3 $/(ton*Km) [52]. It is assumed that the average distance of sludge transportation was 37 km from West Kowloon transfer station to a sludge treatment disposal center in Lung Kwu Tan of Hong Kong (see **Fig. A2**). Combing both operating cost and capital cost, net present value (*NPV*) of the project can be obtained. Because of the time and inflation influence, the cash flow at present is more valuable than that in the future. Therefore, subtracting the discount cash inflow earned in the future from the initial cash outlay required for the investment provides the *NPV* as shown in **Eq. (11)** [49].

$$NPV = \sum_{t=1}^{Life\ span} \frac{AR}{(1+dr)^t} - CAPC \tag{11}$$

Where *AR* is the annual revenue of a project represented by the difference of annual product income and *OPEC*. The discount rate is fixed at 10% for process updates along a life span of 20 years. It is considerable financially worthwhile when the *NPV* of a project is above zero. Moreover, internal rate of return (*IRR*) provides a simper approach to evaluate the potential of project investment for various scenarios. The *IRR* calculation has been shown in **Eq. (12)** and it stands for the discount rate that makes the *NPV* of all cash flows equal to zero. If the *IRR* is higher that the real discount rate, the project displays promising economic feasibility. Also, the production cost of methanol was obtained

by **Eq. (13)**.

$$\sum_{t=1}^{Life\ span} \frac{AR}{(1+IRR)^t} - CAPC = 0 \tag{12}$$

$$Methanol\ cost = \frac{CAPC/20 + OPEC}{Amount} \tag{13}$$

All involved equations for economic evaluation have been summarized in **Table A3**. Nevertheless, limited economic estimation was done here and the accuracy is typically around 30% since the proposed chemical engineering process was studied at a preliminary stage [53].

2.2.2 Environmental evaluation

In this work, a life cycle greenhouse gas (*GHG*) emission was applied to evaluate the environmental performance of the proposed sludge treatment process with methanol production. *GHG* emissions mainly consists of CO_2, CH_4 and N_2O which can be counted as the summarization of direct and indirect emission. Primary energy resources such as coal, crude oil and natura gas were consumed for the utility usage in the gasification-based methanol production process. For example, steam can be produced by burning coals which may generate much greenhouse gas and other pollutants. Herein, it is assumed that steams and required gasifier energy were supplied by the coal combustion. Meanwhile, short-distance transportation by road consumed diesel and gasoline. The energy intensity value was 1362 kJ/(t.km) with an energy consumption of 68% diesel and 32% gasoline [54]. Therefore, *GHG* emissions can be calculated according to the following equations [55].

$$CO_2 = \sum_i \sum_j E_{i,j} (D_{CO_{2,j}} + I_{CO_{2,j}}) \tag{14}$$

$$CH_4 = \sum_i \sum_j E_{i,j} (D_{CH_{4,j}} + I_{CH_{4,j}}) \tag{15}$$

$$NO_2 = \sum_i \sum_j E_{i,j} (D_{NO_{2,j}} + I_{NO_{2,j}}) \tag{16}$$

$$GHG = CO_2 + 23CH_4 + 296N_2O \tag{17}$$

Where $D_{CO2,j}$, $D_{CH4,j}$ and $D_{CO2,j}$ are the direct emissions factors of CO_2, CH_4, and N_2O for process energy j (*i.e.*, electricity, coal, diesel, and gasoline). $I_{CO2,j}$, $I_{CH4,j}$ and $I_{CO2,j}$ are the indirect emissions factors of CO_2, CH_4, and N_2O for process energy. $E_{i,j}$ is the corresponding process energy consumption of unit methanol production. The direct and indirect emission factors of the selected process energy were given in **Table A4**.

2.2.3 Exergy evaluation

The first law of thermodynamics indicates the amount of energy in system and surroundings are

conservative while it treats all the work and heat are equivalent energy without distinguishing them from the energy grade perspective. To overcome the drawbacks in energy analysis, exergy that indicates the maximum theoretical work extractable from heat was calculated in this work. Exergy analysis is an advantageous method compared to conventional energy analysis that can clearly identify the energy loss [56]. Assumptions were made before performing the exergy analysis that dead state is set as 1 atm and 25 ℃ as well as kinetic exergy and potential exergy are neglected. Therefore, only physical exergy and chemical exergy are considered in the material flow (see **Eq. (18)**). As indicated by **Eq. (19)**, the physical exergy is determined by the enthalpy and entropy when setting 1 atm and 25 ℃ as the basis. The physical exergy flow rates can be well obtained using data from ASPEN Plus and a standard spreadsheet calculation program.

$$Ex_{total} = Ex_{ph} + Ex_{ch} \tag{18}$$

$$Ex_{ph} = H - H_0 - T_0(S - S_0) \tag{19}$$

The chemical exergy refers to the maximum work of the considered stream obtainable from the environmental state to the dead state by processes involving heat and mass transfer with the surrounding [57]. The sewage sludge can be seen as a solid fuel, and it only considered chemical exergy because it was introduced under the dead state. The exergy calculation of the sewage sludge was achieved in a similar estimation of the solid fuel based on a recent work [58].

$$Ex_{sludge} = (LHV_{sludge} + 2.442X_M)\cdot\xi + 9417X_S \tag{20}$$

$$\xi = 1.0437 + 0.1882\frac{H}{C} + 0.0610\frac{O}{C} + 0.0404\frac{N}{C} \tag{21}$$

The correlation factor ξ is the ratio of the chemical exergy and the lower heating value of the solid fuel. It depends on the atomic ratios in the sewage sludge feedstocks and can be calculated according to **Eq. (21-22)**. In addition, chemical exergy of a non-gaseous mixture and gas mixture can be defined by the following equations respectively [56].

$$Ex_{ch} = \sum_i n_i Ex_{stand} \tag{23}$$

$$Ex_{ch} = \sum_i x_i Ex_{stand} + RT_0 \sum x_i \ln x_i \tag{24}$$

Where n_i is the mole flowrate of the *ith* component in the stream and x_i refers to the component's molar fraction. R is gas constant that equals to 8.314 KJ/Kmol*K. Ex_{stand} represents the standard chemical exergy of the *ith* component as shown in the **Table A5**. Above all, a complete exergy balance

of controlled system can be formulated as **Eq. (25).**

$$W + \sum Ex_{Q_{in}} + \sum Ex_{in} = \sum Ex_{out} + \sum Ex_{Q_{out}} + \Delta Ex_{loss} \quad (25)$$

Where W is the supplied power or mechanical work, and they are equal to the exergy input. $\sum Ex_{in}$ and $\sum Ex_{out}$ denote the exergy flow associated with inflowing and outflowing materials, respectively. While $\sum Ex_{Q_{in}}$ and $\sum Ex_{Q_{out}}$ are the utility heat source and sink, respectively. Both are rested on heat temperature and transferred heat duty Q_i, which can be calculated by **Eq. (26)**. Exergy loss ΔEx_{loss} is caused by the irreversible nature of real processes.

$$Ex_Q = \sum_i \left((1 - \frac{T_0}{T_i}) Q_i \right) \quad (26)$$

Finally, exergy efficiency of a typical chemical engineering process is defined as the ratio of output exergy and the input exergy.

$$\eta = \frac{Ex_{product}}{Ex_{sludge} + Ex_{add}} \quad (27)$$

3. Results and discussion

3.1 Gasification results

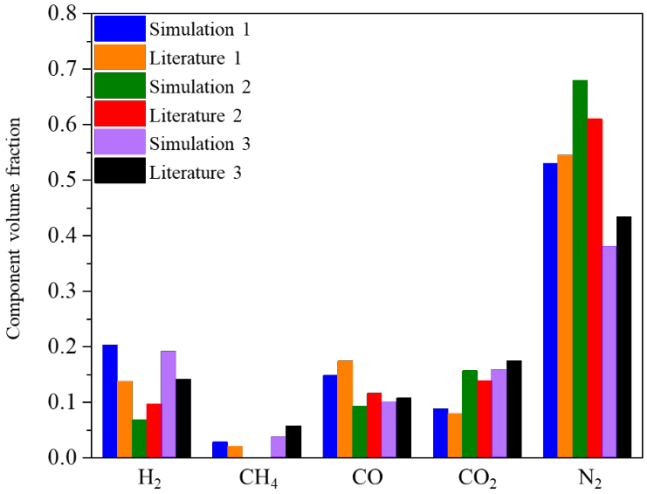

Fig. 2. Gasification model validation in terms of the major syngas compositions under various conditions

The gasification model was verified by comparing simulation data with the experimental results under the same operation conditions in literature 1 [28] (ER=0.28, Temperature=781 ℃ and Moisture content =6.4%). In general, the gasification simulation using equilibrium model could be seen as acceptable when the calculated average relative error (ARE) is less than 20% [35, 36]. Herein, ARE

was computed as 18.63% by **Eq. (28)**. It was observed from **Fig. 2** that the model prediction was globally in good agreement with the experimental results although the N_2 gas has a large deviation from the experimental results. In this case, the restricted chemical equilibrium model for the gasification was built up with manually setting the temperature approach for R1-R5 shown in **Table 2** equals to -150, -195, 60, -200 and 50 ℃, respectively.

$$ARE = \frac{1}{m}\sum_{i}^{m}\left|\frac{y_m - y_e}{y_e}\right| \tag{28}$$

Where y_m and y_e were simulation and experimental results in terms of the corresponding specified components of major gasification gas products. Considering that the uncertainty and error of experimental data may also affect the performance of model verification, the gasification model was double verified by other experiments to ensure the effectiveness of the calculation results. Same operation conditions of the literature 2 (i.e., gasifier temperature was 800 ℃ with feedstock sludge 6 kg/h and air flowrate 8.95 kg/h) [59] were employed in the simulation 2. Moreover, the gasification conditions of biosolid in literature 3 [34] was 780 ℃ with feedstock sludge 7.05 kg/h and air flowrate 5.2 kg/h. The comparison results of simulation model were also displayed in **Fig. 2**. It could be observed that the predicted results are in good agreement with the reported data (ARE=19.69% and 19.45%, respectively).

After obtaining the restricted equilibrium model parameters, we further investigate the impacts of gasification operational factors like mass moisture content, air equivalent ratio (*ER*) and gasification temperature. Moisture content can affect the equilibrium of gasification reactions and higher temperature required more external energy addition. *ER* is the ratio between the actual air molar quantity and the theoretical air supply for complete combustion. For a given sludge feedstock with specified ultimate results, the assumed composition can be written as $CH_aO_bN_cS_d$ then *ER* can be calculated by the following equation.

$$ER = \frac{m}{(1 + a/4 - b/2 + c + d)\times 4.76} \tag{29}$$

Where *m* is the actual molar flowrate of air supplement. In the sensitivity analysis, the influences of above-mentioned factors on the H_2 production, syngas composition, lower heating value (*LHV*) of syngas and cold gas efficiency (*CGE*) were investigated. The *LHV* (MJ/Nm^3) of product gas depends on the volume percentage of CO, H_2 and CH_4 in the raw syngas and can be obtained through **Eq. (30)**

[60]. The *CGE* is defined as the ratio of the flow of energy in the syngas and the energy contained within the feedstock sludge (See **Eq. (31)**).

$$LHV_{gas} = 35.88x_{CH_4} + 12.63x_{CO} + 10.78x_{H_2} \quad (30)$$

$$CGE(\%) = \frac{v_{gas} \times LHV_{syngas}}{M_{sludge} \times LHV_{sludge}} \quad (31)$$

Where x is the volume fraction of gas products after the gasification reaction. v_{gas} is the total volume (Nm^3) of CO, H_2 and CH_4. The value of LHV_{sludge} is 25.63 MJ/kg according to the study [32].

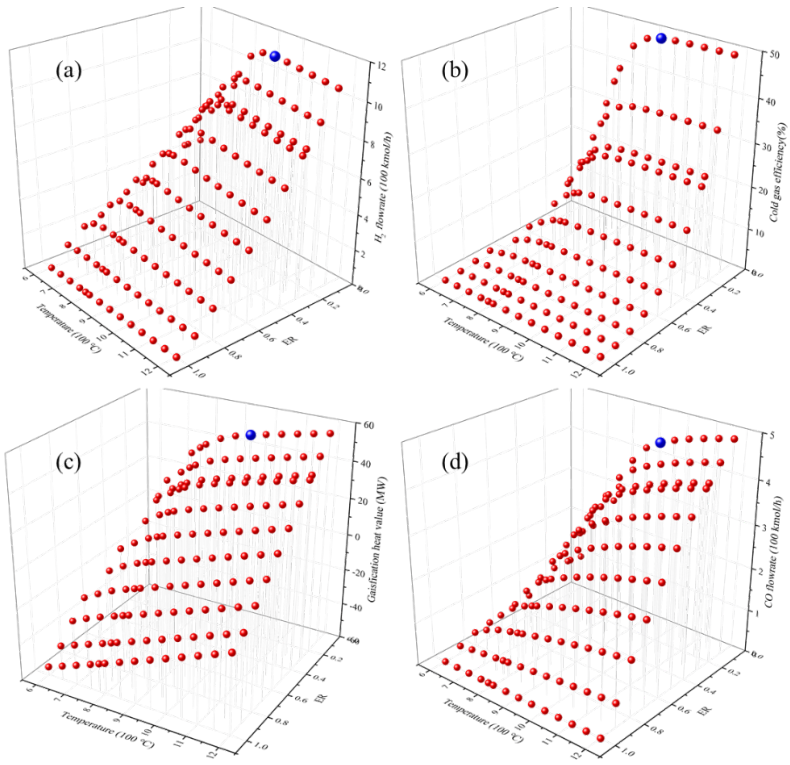

Fig. 3. The influence of gasification temperature and air flowrate on (a) the H_2 flowrate; (b) the CGE performance; (c) gasification energy consumption; and (d) CO flowrate.

Three major variables namely the gasification temperature, *ER* and the moisture content were changed to investigate the metrics variation of produced H_2, CO, the CGE and gasification energy consumption. The gasification temperature was ranged from 600 to 1200 ℃. *ER* value was changed from 0.1 to 1.0. Moreover, moisture content was adjusted from 0 to 60%. Three variables were simultaneously changed in the simulation and the optimal operation conditions in terms of the largest amount of hydrogen flowrate were *ER*=0.1, 950 ℃ and 60 % moisture content which was shown in blud balls in the following **Fig. 3** and **4**. It can be observed from **Fig. 3** that blue balls in each subplot were not always the optimal results. Nevertheless, the amount of H_2 gas was set as the objective of

sensitivity analysis because the hydrogen gas plays an important role in the methanol synthesis. As shown in **Fig. 3(a)**, with the decreasing air flowrate, more hydrogen can be produced from the gasifier. This may be caused by the water gas shift reaction under the condition of more carbon monoxide that produced by partial oxidation of carbon solid. Also, **Fig. 3(a)** reveals that higher temperature is beneficial for hydrogen production. *CGE* is a key metrics for evaluating the performance of energy conversion during the gasification. Generally, if more combustible components like H_2, CH_4 and CO was generated then much higher *CGE* will be in display. The trend of *CGE* resembles that of H_2 and CO flowrate. This may be ascribed to the dominated amount of H_2 and CO gases. The gasification heat value equals to the heat summarization of drying, pyrolysis and gasification subsections. It was implied from **Fig. 3(c)** that the complete combustion with enough air will release much heat and thus the total gasification heat duty shown a negative value.

Fig. 4 was dedicated to demonstrating the influence of moisture content on four indicators H_2 flowrate, CO flowrate, *CGE* and energy consumption. Higher moisture content favours in the hydrogen production while poses a converse effect on the CO generation. In addition, it needs more energy consumption during the gasification section because of the endothermic nature of water gas reaction and Boudouard reaction in the gasification process. As shown in **Fig. 4**, the bule ball cannot represent the best CGE and CO flowrate, nor the minimized total energy consumption. However, the blue ball stands for the maximum H_2 flowrate which is a key factor influencing the methanol synthesis. To some extent, the sewage sludge gasification provides a renewable approach for the H_2 production since H_2 was mainly obtained through the natural gas reforming or electrolytic water [61].

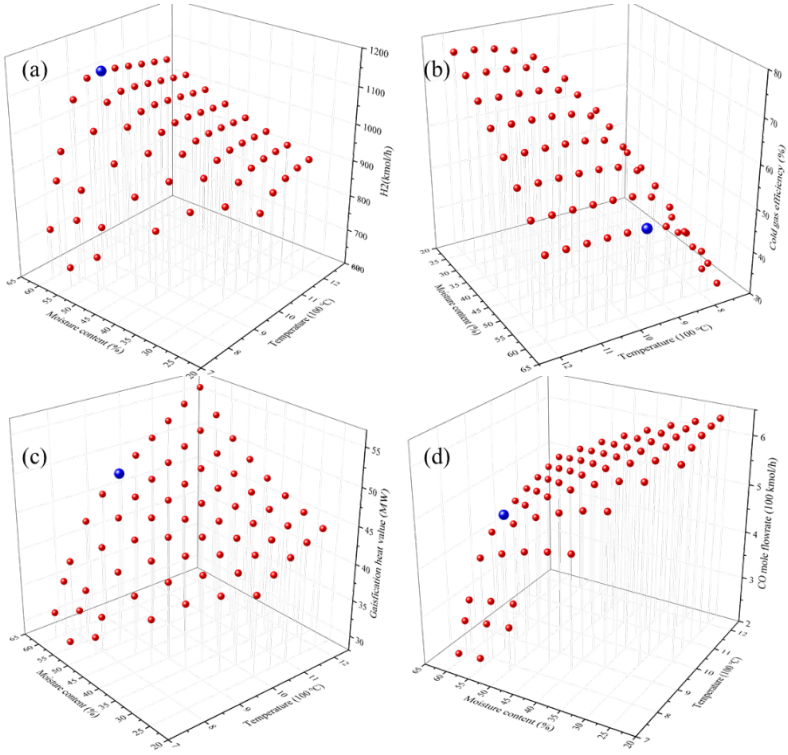

Fig. 4. The influence of gasification temperature and moisture content on (a) the H_2 flowrate; (b) the CGE performance; (c) gasification energy consumption; and (d) CO flowrate.

3.2 Power generation analysis

To recover heat energy from the high-temperature stream, steam cycle power generations were implemented in this work. Some essential factors namely the water flowrate, cold stream outlet temperature, discharged pressures of pump and steam turbine greatly influence the power generation. Firstly, the flowrate of water and superheat degree of steam were adjusted to achieve the largest value of heat duty. It represented the maximum heat recovery from the crude syngas stream. Then, the discharged pressures of the pump and steam turbine was adjusted to obtain a maximum brake work of steam turbine. It must be noted that some results from the sensitivity analysis of the power generation shown the temperature cross in the heat-exchanger simulation, thus these points should be deleted. The sensitivity analysis for two power generation subprocesses were given in **Fig. 5** and **6**, respectively. The first steam cycle process was used to recover heat energy from raw syngas. The cycled water flowrate was adjusted from 1800 to 1850 kmol/h and the superheat degree of outlet steam was varied in a range from 1 to 15 ℃. In addition, the discharge pressure of pump and steam turbine were set in ranges 40-54 atm and 0.92-1.20 atm, respectively.

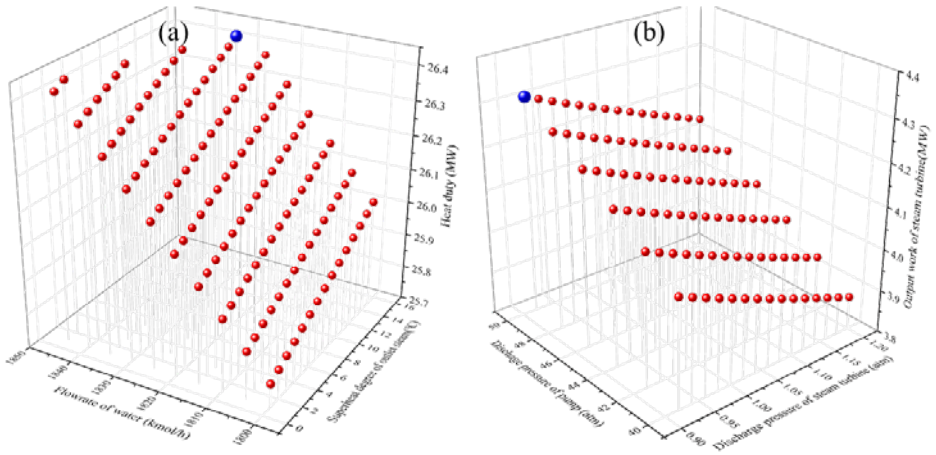

Fig. 5. (a) The influence of water flowrate and superheat degree of steam on the heat duty of recycled energy; (b) The influence of discharge pressures of pump and steam turbine on the produced work

As shown in **Fig. 5(a)**, the blue ball represents the optimal condition associated with a water flowrate of 1830 kmol/h and a superheat degree of steam of 14 ℃. Actually, larger water flowrate and steam temperature will recovery more heat energy from raw syngas. However, it is limited by the heat exchanger operating with no temperature cross. Then, maximum power generation was given under the largest pressure difference between the pump (*i.e.*, 50 atm) and steam turbine (*i.e.*, 0.9 atm).

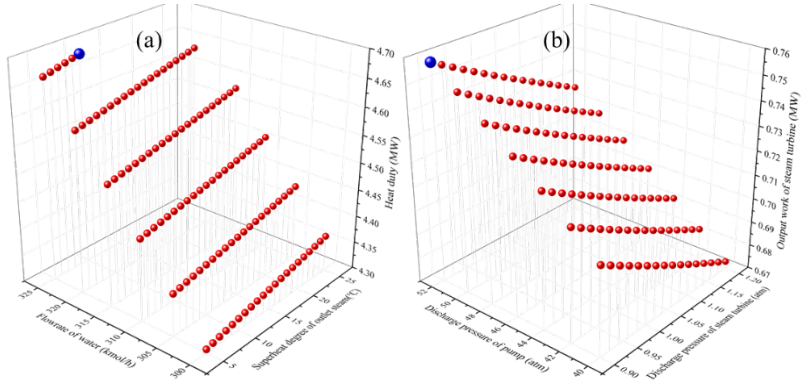

Fig. 6. (a) The influence of water flowrate and superheat degree of steam on the heat duty of recycled energy; (b) The influence of discharge pressures of pump and steam turbine on the produced work

Before the raw syngas was introduced into the absorption column, it should be compressed and cooled to a suitable condition for efficient removal of acid gas. Therefore, another steam cycle process can be used to recover the heat energy. The water flowrate in the cycle varied from 300 to 325 kmol/h and the superheat degree of outlet steam was changed from 5 to 25 ℃. Furthermore, the discharge pressure of pump and steam turbine were set in ranges 40-52 atm and 0.90-1.20 atm, respectively. The sensitivity analysis results were shown in **Fig. 6**. It reveals that the optimal conditions for maximum

recovered heat were 320 kmol/h water flowrate and superheat degree of 10 ℃. They are less compared to that in the first steam process. The obtained pressures of pump and steam turbine in the second power generation section were 52 atm and 0.9 atm.

3.3 Absorption process

The major aim of this section is to remove most of H_2S component from the syngas and obtain the clean gas for methanol synthesis. And a low temperature and high pressure is good for the gas-liquid solubility as well as the absorption. The raw syngas was sent into the top of absorption column at 10 atm and 35 ℃. The design specification of absorption column was provided in **Table A6**. In general, two key factors namely circulation rate and the concentration of MDEA solution greatly affect the H_2S removal efficiency. To optimize the operation parameters, the ratio of circulation rate to feed raw syngas (L/G) was varied from 0.1 to 1.0 under the fixed 5 mol% MDEA concentration. Then, the MDEA concentration was changed from 1 mol% to 10 mol% targeting on investigating the H_2S removal efficiency. The sensitivity analysis results have been shown in **Fig. A3**. Results indicated that increased L/G ratio and MDEA concentration is benefit for removing H_2S substance. It should be noted that the H_2S in feedstock only account for 0.12 mol% of the raw syngas. Therefore, it can be readily achieved to obtain 99.99% removal when L/G larger than 0.5 and MDEA concentration larger than 5 mol%. In this regard, the L/G and MDEA concentration were selected as 0.5 and 5 mol%.

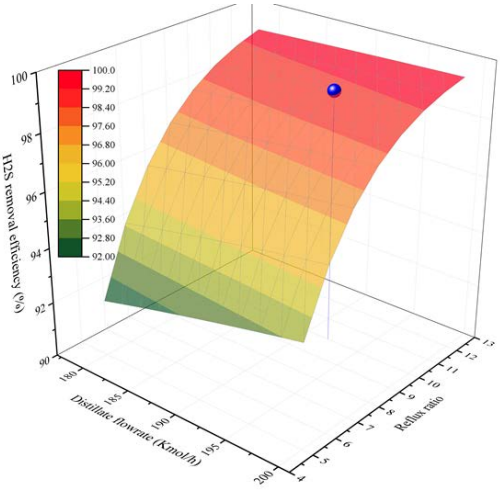

Fig. 7. The effect of reflux ratio and distillate flowrate on the H_2S removal efficiency of the stripper column

After the absorption column, the bottom stream that contains H_2S component with 2.5591 kmol/h was sent into the regeneration stripper column. The regeneration column was maintained at lower pressure and high temperature due to advantages in distillation. The pressure of stripper column is 1 atm. And a heat exchanger was used to raise the feed temperature to 85℃. This preheating

configuration can decrease the reboiler duty of regeneration column. Different from the absorber column, a vapor-liquid equilibrium model was used in the stripper. Considering the energy consumption, we set the molar recovery of H_2S as 99% which means at least 2.5335 kmol/h H_2S should be collected from the top of stripper column. Then, an analysis was conducted with respect to the influence of reflux ratio and distillate flowrate on the H_2S removal efficiency. As shown in **Fig. 7**, both reflux ratio and distillate flowrate do a favour in increasing the H_2S removal efficiency. However, higher efficiency means more reboiler duty for the separation. Moderate 99% of H_2S recovery was selected (see blue ball in **Fig. 7** and the corresponding condition was given associated with distilled flowrate of 192 kmol/h and reflux ratio of 10. Then, the total number of stages was 15 which was chosen based on the convergence requirement of simulations. **Fig. 8** has shown the detailed information of the absorption process. Molar flowrate of related ion components was not displayed individually. Apparent flowrate was given in **Fig. 8** to better demonstrate the electrolyte system.

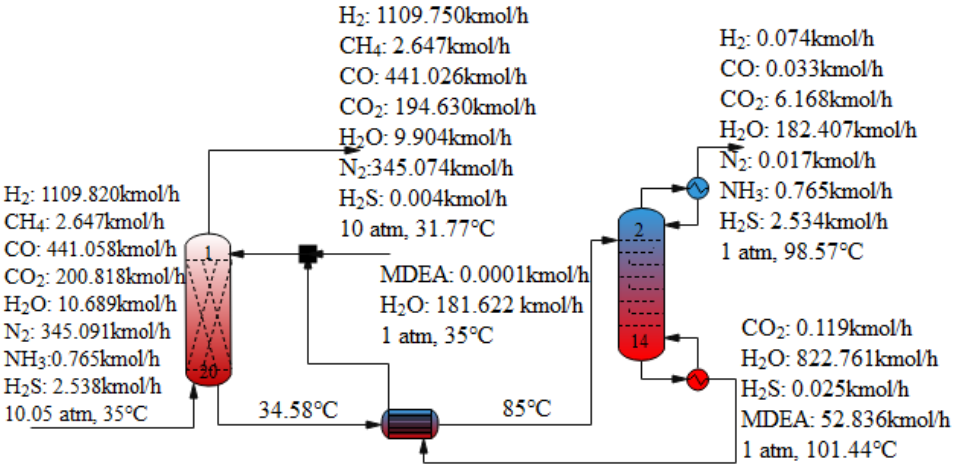

Fig. 8. The absorption process flowsheet with apparent molar flowrate

3.4 Methanol process

The methanol synthesis was a mature technology, and the simulation was finished according to the methodology demonstration in **Section 2.1**. The pressure and temperature in methanol synthesis reactor were chosen as 75 atm and 240 ℃ [45, 62]. RK-SOAVE equation of state was applied in calculating related physical chemistry parameters. A fraction of recycled gas during the synthesis was purged to avoid gas cumulation. Obtained crude methanol with detailed compositions was given in **Table A7**. It is evident that major impurities come from the water and other light gas. It is required to make a purification and thus two equilibrium-based distillation columns were applied. The first distillation column aimed at separating most light gas from the mixture. With varying the distillate

flowrate, the molar recovery of CO_2 can be achieved above 99.9%. Meanwhile, the sensitivity analysis was conducted to investigate the influence of reflux ratio on the final reboiler duty of the first distillation column (see **Fig. A4**). The optimal reflux ratio is found to be 0.1 associated with a distillate flowrate of 88.913 kmol/h. Because a refrigerant utility with -25 ℃ temperature was used for partial condensation of low-temperature light gas. The column pressure was adjusted at 20 atm to meet the heat-transfer requirement.

Second distillation column operated at the atmospheric pressure was used to separate water and methanol. Operating at 1 atm can guarantee the cooling water useful for the condenser. Different from the analysis of the first distillation column, the methanol purity should be considered as well. As such two design specifications were set to control the methanol recovery (99.9%) and its purity (99.9%) by changing the distillate flowrate and reflux ratio, respectively. Eventually, the obtained distillate rate and reflux ratio were 490.076 kmol/h and 1.109. In addition, Suitable number of stages and feed stages of two distillation columns were set according to the temperature profiles of two columns. As shown in **Fig. 9 (a)** and **(b)**, each plate in both distillation columns caused separation effects with clear temperature variations. It was evident from **Fig. 9 (c)** that few light gasses existed in the bottom of distillation column C1 and the feed stage is 4th tray. Since there is no azeotrope the distillation column C2 can well obtained methanol product with 99.9 mol% purity. The column profiles indicated both distillation columns were well optimized.

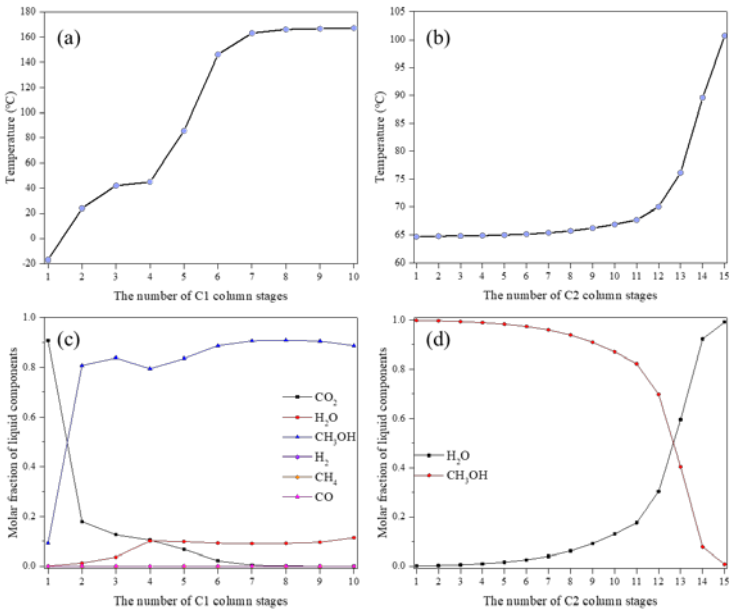

Fig. 9. (a) (b) Temperature profiles and (c) (d) major liquid composition in distillation column C1 and C2

3.5 Economic, environmental and exergy analysis

3.3.1 Economic results

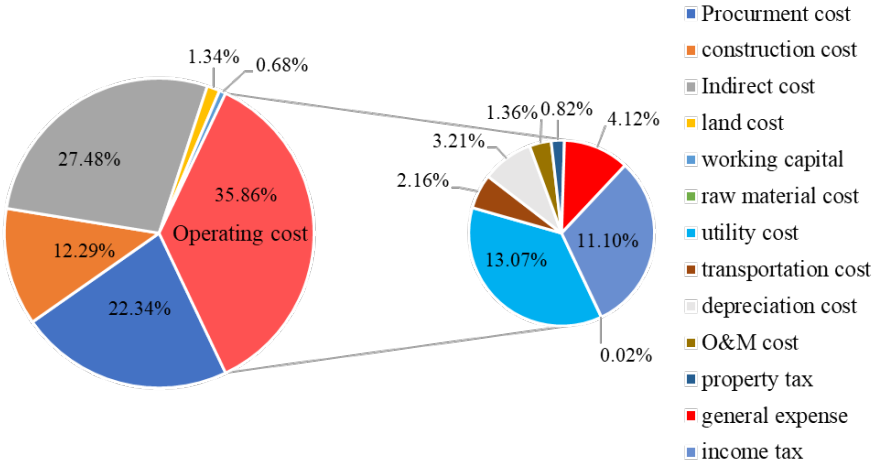

Fig. 10. Economic cost breakdown for the gasification process

Through the sensitivity analysis of key variables in different subsections, detailed streams mass flowrates have been obtained and summarized in **Appendix B**. Followed by a sustainability analysis in terms of different aspects, whether if the STM plant is promising should be answered. Detailed estimation cost of the STM process was shown in **Table A8**. The economic cost breakdown for the *CAPC* and *OPEC* of the initial gasification was shown in **Fig. 10**. It was shown that *OPEC* accounts for only 35.86% of the total cost and the remain 64.14% of the total cost was the *CAPC*. This was in accord with the practical chemical engineering plant. Large amount of initial investment was the equipment related cost (*i.e., CAPC*). Indirect cost (25.24 million $) which includes miscellaneous overhead, field services, labour benefits and et al dominated the *CAPC* followed by the equipment procurement (131.73 million $) and construction cost (45.89 million $). The right pie chart displayed the breakdown of *OPEC* and it revealed that utility consumption and income tax was the major cost contributor which takes up 13.07% and 11.10%, respectively. The price of involved chemicals and utility energy has been given in **Table A9**. Notably, pure nitrogen gas was separated from a pressure-swing adsorption equipment and the referred price of nitrogen gas product was 0.00123/m^3 at a condition of 15 Mpa and 25 ℃.

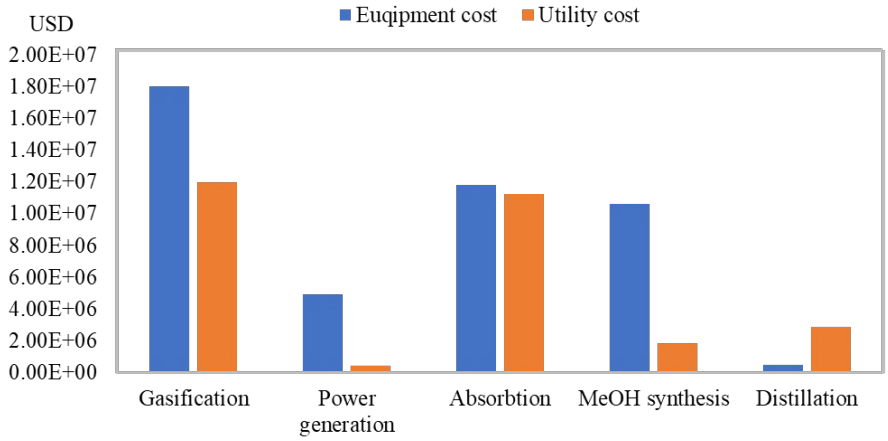

Fig. 11. Equipment cost and utility cost of subsections of the proposed conversion process

To make a clearer comparison of subsections in the process, we then calculated the equipment and utility cost in different subprocesses. As shown in **Fig. 11**, there is no doubt that the gasifier system consumed the largest energy to maintain the required gasification state of high temperature condition. The equipment procurement cost in the gasification section was 18.04 million$ and the gasification consumed a high-temperature fuel cost for 12 million$. It was implied from the calculation that the gasification system in the proposed system still has the potential to be further optimized. Absorption process is second largest expensive in terms of the equipment cost (11.79 million$) because it included a costly compressor. Moreover, the procurement cost (10.60 million$) of methanol synthesis has a similar value of that of absorption process. In terms of the methanol distillation, the process did consume high-pressure steam in the reboiler and low-temperature refrigerant in the condenser. The utility usage is much lower compared with that in the gasification system.

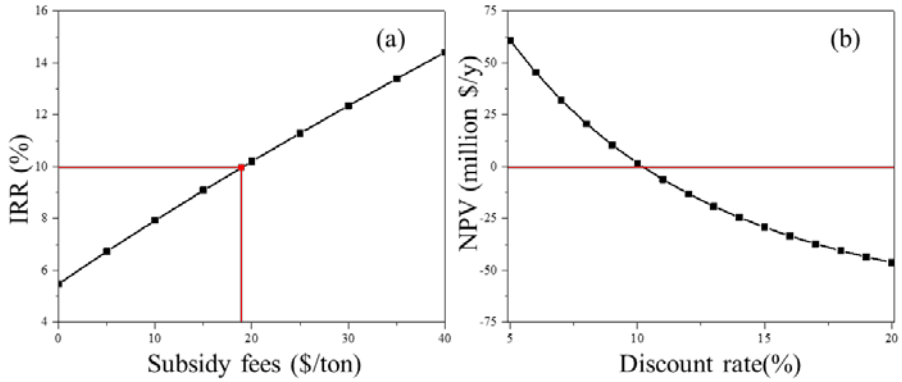

Fig. 12. (a) the effect of subsidy level on the final IRR of the project and (b) the effect of discount rate on the NPV of the project in 20 years life span

The calculated cost of sewage sludge gasification-based treatment is 39.58 $/ton which is lower than the conventional sludge treatment by combustion in China mainland (approximately 61.54-76.92

$/ton [63]). The methanol production cost by proposed STM process was 579.62 $/ton, and this value is in accord with that in the recent summary report by International Renewable Energy Agency (*i.e.*, 400-800 $/ton) [64]. Nevertheless, as shown in **Table A8**, it is hard for the proposed STM plant to achieve beneficial economics in the case of no subsides provided by local government as the *NPV* value is negative based on assumed 10% discount rate. Meanwhile, calculated *IRR* value is only 5.48% representing the critical value of discount rate that makes *NPV* equal to zero. To better understand the importance of public financial support, **Fig. 12 (a)** have shown the influence of subsidy fees on the final *IRR*. Notably, the analysis was conducted under the assumption of no price fluctuations of methanol and by-product nitrogen. It was indicated from **Fig. 12 (a)** that an increased subsidy support does a favour in the economic benefits. Generally, 10% of *IRR* is used as a good value to evaluate the economic feasibility of a project when considering the currency inflation. In light of this, a subsidy of 20 $/ton could be suitable for the STM plant implementation.

On the other hand, the price of methanol produced in this way is relatively high. Therefore, the effect of methanol price fluctuation on the economic indicator *IRR* should be further conducted to identify the feasibility of STM process. To evaluate this influence, the sensitivity analysis method was performed by giving a variation of ±20% in the methanol price. **Fig. A5** has shown the analysis results and the basic methanol price is set as 450 $/ton. When the methanol price is more than 461.68 $/ton under the circumstance of no subsidy fees, the project was economically feasible. This is in accordance with the negative *NPV* value that shown in **Table A8**. After 20 $/ton support is given, the project will be economically doable when methanol price is more than 403.88 $/ton. With the increased methanol price, the project becomes more profitable.

Fig. 12 (b) has reflected the influence of discount rate on the *NPV* when giving a subsidy of 20$/ton. In this case, if the actual discount rate is much larger than 10%, total cash flow in 20 years will be negative which means the project conduction would be not doable. The discount rate can be refereed as the interest rate charged to commercial banks and other financial institutions for short-term business loans. According to the statistics of business bank in Hong Kong [65], average interest rate of 6.5% was shown in the past 40 years. Therefore, it was indicated from **Fig. 12 (b)** that a subsidy of 20$/ton associated with 6.5% discount rate was enough for achieving the positive *NPV*. In summary, the STM project with sludge disposal capacity of 1200 ton/day is promising in the economic aspect at a cost of public support. At the initial stage of a new greener technology, this kind of public support is

an effective method to promote a greener and circular economy.

3.3.3 Environmental results

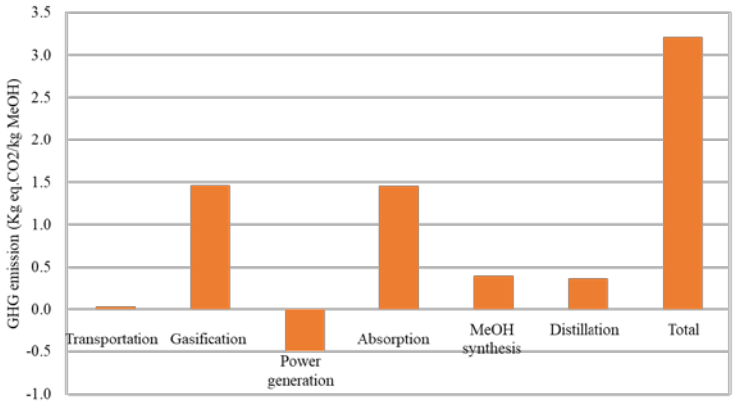

Fig. 13. Life cycle GHG emissions of subprocesses for the proposed methanol production

LCA environmental analysis of the proposed process was performed using the simulation results according to **Eq. (14-17)** and corresponding emission factors. The function unit was 1kg produced methanol. Eventually, **Fig. 13** has given the GHG emissions of subsections for the STM process. The total GHG emission of the methanol production from the treatment of sludge was 3.21kg eq.CO_2. Relatively large GHG emissions were shown in the gasification and absorption sections. The GHG emission of gasification and absorption subsections were 1.47 and 1.45 kg eq.CO_2, respectively. It is evident that power generation section can mitigate the carbon emission by 0.50 kg eq.CO_2. The net carbon reduction of power generation is limited. To some extent, gasification and absorption process accounts for large carbon emissions which implies the bottleneck of further improvement. To reduce the environmental pollution and conform to the low-carbon manufacturing, future research is necessary to explore the energy integration network to reduce the GHG emissions caused by the utility consumption of gasification units.

3.3.2 Exergy results

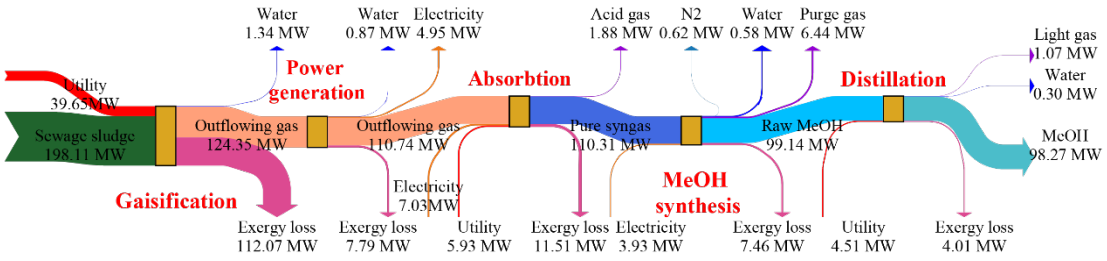

Fig. 14. The exergy flow of the STM treatment process

According to a sludge to methanol study which focus on the energy efficiency [66], the overall exergy efficiency is about 53%. For the proposed processes, the exergy streams of the system have

been shown in **Fig. 14**. Only methanol was set as the product and the calculated exergy efficiency was 37.92%. The total exergy input is about 259.16 MW which including the utility input and sewage sludge exergy. During the gasification-based utilization process, the air gasification system has the largest exergy destruction (*i.e.*, 112.07 MW) followed by the absorption system (*i.e.*, 11.51 MW). The exergy loss during the methanol synthesis section is 7.46 MW and it accounts for 5.22% of the total exergy destruction while during gasification accounts for 78.46%. The detailed distribution of exergy destruction was given in **Fig. A6**. A reason for the largest exergy loss in gasification was the high-temperature condition associated with high irreversibility of chemical reactions. In summary, further improvement can be carried out by focusing on increasing the energy efficiency of gasification and absorption sections through the process system engineering technology.

4. Conclusion

A sludge-to-methanol process was conceptually designed by considering the case in Hong Kong. Based on the detailed simulation in Aspen Plus, sensitivity analysis of key operational parameters was conducted such as gasification temperature, ER and moisture content after the validation of the restricted Gibbs equilibrium gasification model. Economic results revealed the IRR of the STM plant is 5.48% under the scenario of no subsidy support. The sludge disposal cost and methanol production cost were 39.58 and 579.62$/ton, respectively. An averaged IRR value of 10% is appropriate for the economic feasible thus a subsidy of 20$/ton sludge should be given to obtain a positive NPV. In addition, the total lifecycle GHG emission is 3.21 kg eq.CO_2/kg methanol. GHG emissions of the gasification section is the largest because of the high temperature condition should be maintained by consuming lots of utility coals. The overall exergy efficiency of STM is 37.92% and relatively dominated proportion of exergy loss was shown in the gasification and absorption, which indicated both subsections still have room for further improvement. In terms of the practical implication, this work can give some guidelines for the gasification utilization of sludge in Hong Kong. It is implied from the exergy analysis that how to improve the energy efficiency of sludge gasification and the syngas cleaning should be the future focus which may involve more pilot-scale experiments and energy integration network design. Economic analysis indicated the commercial start-up of this plant was not easy. Public subsidy must be given to the plants to support the technical retrofit and future innovation. Detailed environmental impacts comparison was not studied in this research while we provided a GHG

emission value for the reference. In the near future, a detailed comparative life cycle research should be conducted to show how good of the STM process is when compared to conventional methanol production processes. During the environmental comparison analysis, it is also considerable to involve the carbon tax concept.

It should be noted that the model construction of the sewage sludge to methanol conversion was finished based on the restricted thermodynamic equilibrium model. This Aspen Plus model conducted the complex gasification process simulation in a simpler way as the small sections (e.g., pyrolysis, gasification and fully combustion) in the gasification were tested and adjusted individually. Therefore, it does not need to cover all the chemical reactions in complex reacting systems. These advantages have contributed to the wide application of equilibrium models in the design and evaluation of solid coal gasification especially happened in the large-scale downdraft gasifier. However, the weakness of the applied model is obvious. Some assumptions like that tar were not considered and the heat loss was neglected were firstly given to simplify the gasification-based methanol production models. Those assumptions may not practically be accurate to reproduce all the experimental results. Further improvement should be made in the model accuracy by considering artificial neutral network models and detailed kinetic models.

Declaration of Competing Interest

The authors declare that they have no known competing financial interests or personal relationships that could have appeared to influence the work reported in this paper.

Acknowledgement

The work described in this paper was supported by the grant from the Research Committee of The Hong Kong Polytechnic University under student account code RK3P and was also financially supported by the Hong Kong Research Grants Council for Early Career Scheme (Grand No. 25208118, Project ID. P0006219, Funding Body Ref. No. PolyU 252081/18E).

Appendix

The Supplementary material is available free of charge via the Internet.

Reference

[1] J. Qu, H. Wang, K. Wang, G. Yu, B. Ke, H.-Q. Yu, et al. Municipal wastewater treatment in China: Development history and future perspectives. Frontiers of Environmental Science & Engineering. 13 (2019) 88.

[2] L. Zhang, C.C. Xu, P. Champagne, W. Mabee. Overview of current biological and thermo-chemical treatment technologies for sustainable sludge management. Waste Manag Res. 32 (2014) 586-600.
[3] Environmental Protection Department, Sewage Sludge Intake, Sewage Sludge Collected by the Sludge Treatment Facility. 2022, Avaliable: https://wwwepdgovhk/epd/english/environmentinhk/waste/data/sludge_intakehtml.
[4] Y. Liu, R. Lin, Y. Man, J. Ren. Recent developments of hydrogen production from sewage sludge by biological and thermochemical process. International Journal of Hydrogen Energy. 44 (2019) 19676-97.
[5] I.L. Motta, N.T. Miranda, R. Maciel Filho, M.R. Wolf Maciel. Sugarcane bagasse gasification: Simulation and analysis of different operating parameters, fluidizing media, and gasifier types. Biomass and Bioenergy. 122 (2019) 433-45.
[6] D. Selvatico, A. Lanzini, M. Santarelli. Low Temperature Fischer-Tropsch fuels from syngas: Kinetic modeling and process simulation of different plant configurations. Fuel. 186 (2016) 544-60.
[7] M. Fernandez-Lopez, J. Pedroche, J.L. Valverde, L. Sanchez-Silva. Simulation of the gasification of animal wastes in a dual gasifier using Aspen Plus®. Energy Conversion and Management. 140 (2017) 211-7.
[8] U. Lee, J. Dong, J.N. Chung. Experimental investigation of sewage sludge solid waste conversion to syngas using high temperature steam gasification. Energy Conversion and Management. 158 (2018) 430-6.
[9] M. Imbierowicz, A. Chacuk. Kinetic model of excess activated sludge thermohydrolysis. Water Research. 46 (2012) 5747-55.
[10] C. He, A. Giannis, J.-Y. Wang. Conversion of sewage sludge to clean solid fuel using hydrothermal carbonization: Hydrochar fuel characteristics and combustion behavior. Applied Energy. 111 (2013) 257-66.
[11] C. Freda, G. Cornacchia, A. Romanelli, V. Valerio, M. Grieco. Sewage sludge gasification in a bench scale rotary kiln. Fuel. 212 (2018) 88-94.
[12] D. Hantoko, M. Yan, B. Prabowo, H. Susanto, X. Li, C. Chen. Chapter 13 - Aspen Plus Modeling Approach in Solid Waste Gasification. in: S. Kumar, R. Kumar, A. Pandey, (Eds.), Current Developments in Biotechnology and Bioengineering. Elsevier2019. pp. 259-81.
[13] D. Hantoko, H. Su, M. Yan, E. Kanchanatip, H. Susanto, G. Wang, et al. Thermodynamic study on the integrated supercritical water gasification with reforming process for hydrogen production: Effects of operating parameters. International Journal of Hydrogen Energy. 43 (2018) 17620-32.
[14] F. Zhang, S. Wang, Y. Li, W. Chen, L. Qian. Thermodynamic analysis of a supercritical water gasification – oxidation combined system for sewage sludge treatment with cool wall reactor. Energy Conversion and Management. 247 (2021).
[15] R. Bijesh, P. Arun, C. Muraleedharan. Modified stoichiometric equilibrium model for sewage sludge gasification and its validation based on experiments in a downdraft gasifier. Biomass Conversion and Biorefinery. (2021).
[16] Q. Yang, H. Zhou, P. Bartocci, F. Fantozzi, O. Mašek, F.A. Agblevor, et al. Prospective contributions of biomass pyrolysis to China's 2050 carbon reduction and renewable energy goals. Nature Communications. 12 (2021) 1698.
[17] F. Dalena, A. Senatore, A. Marino, A. Gordano, M. Basile, A. Basile. Chapter 1 - Methanol Production and Applications: An Overview. in: A. Basile, F. Dalena, (Eds.), Methanol. Elsevier2018. pp. 3-28.
[18] M. Blug, J. Leker, L. Plass, A. Günther. Methanol Generation Economics. in: M. Bertau, H. Offermanns, L. Plass, F. Schmidt, H.-J. Wernicke, (Eds.), Methanol: The Basic Chemical and Energy Feedstock of the Future: Asinger's Vision Today. Springer Berlin Heidelberg, Berlin, Heidelberg, 2014. pp. 603-18.
[19] B. Hernández, M. Martín. Optimal Process Operation for Biogas Reforming to Methanol: Effects of Dry Reforming and Biogas Composition. Industrial & Engineering Chemistry Research. 55 (2016) 6677-85.
[20] R.O.d. Santos, L.d.S. Santos, D.M. Prata. Simulation and optimization of a methanol synthesis process from different biogas sources. Journal of Cleaner Production. 186 (2018) 821-30.
[21] M. Puig-Gamero, J. Argudo-Santamaria, J.L. Valverde, P. Sánchez, L. Sanchez-Silva. Three integrated process simulation using aspen plus®: Pine gasification, syngas cleaning and methanol synthesis. Energy Conversion and Management. 177 (2018) 416-27.

[22] K. Im-orb, A.N. Phan, A. Arpornwichanop. Bio-methanol production from oil palm residues: A thermodynamic analysis. Energy Conversion and Management. 226 (2020).
[23] P.L. Cruz, D. Iribarren, J. Dufour. Exergy analysis of alternative configurations of a system coproducing synthetic fuels and electricity via biomass gasification, Fischer-Tropsch synthesis and a combined-cycle scheme. Fuel. 194 (2017) 375-94.
[24] M. Del Grosso, B. Sridharan, C. Tsekos, S. Klein, W. de Jong. A modelling based study on the integration of 10 MWth indirect torrefied biomass gasification, methanol and power production. Biomass and Bioenergy. 136 (2020).
[25] Q. Yang, S. Xu, Q. Yang, D. Zhang, Z. Li, H. Zhou, et al. Optimal design and exergy analysis of biomass-to-ethylene glycol process. Bioresour Technol. 316 (2020) 123972.
[26] L. Menin, V. Benedetti, F. Patuzzi, M. Baratieri. Techno-economic modeling of an integrated biomethane-biomethanol production process via biomass gasification, electrolysis, biomethanation, and catalytic methanol synthesis. Biomass Conversion and Biorefinery. (2020).
[27] H. Qi, P. Cui, Z. Liu, Z. Xu, D. Yao, Y. Wang, et al. Conceptual design and comprehensive analysis for novel municipal sludge gasification-based hydrogen production via plasma gasifier. Energy Conversion and Management. 245 (2021).
[28] O. Alves, L. Calado, R.M. Panizio, M. Goncalves, E. Monteiro, P. Brito. Techno-economic study for a gasification plant processing residues of sewage sludge and solid recovered fuels. Waste Manag. 131 (2021) 148-62.
[29] E. Medina-Martos, I.-R. Istrate, J.A. Villamil, J.-L. Gálvez-Martos, J. Dufour, Á.F. Mohedano. Techno-economic and life cycle assessment of an integrated hydrothermal carbonization system for sewage sludge. Journal of Cleaner Production. 277 (2020).
[30] H. Shahbeig, M. Nosrati. Pyrolysis of municipal sewage sludge for bioenergy production: Thermo-kinetic studies, evolved gas analysis, and techno-socio-economic assessment. Renewable and Sustainable Energy Reviews. 119 (2020).
[31] A. AlNouss, M. Shahbaz, G. McKay, T. Al-Ansari. Bio-methanol production from palm wastes steam gasification with application of CaO for CO2 capture: techno-economic-environmental analysis. Journal of Cleaner Production. 341 (2022) 130849.
[32] J.A. Shao, H. Chen, X. Dai, H. Yang. Experiment of pyrolytic characteristics of sewage sludge from Hongkong. Journal of Huazhong University of Science and Technology (Natural Science Edition). 5 (2009) 120-4.
[33] J. Han, Y. Liang, J. Hu, L. Qin, J. Street, Y. Lu, et al. Modeling downdraft biomass gasification process by restricting chemical reaction equilibrium with Aspen Plus. Energy Conversion and Management. 153 (2017) 641-8.
[34] A. Abdelrahim, P. Brachi, G. Ruoppolo, S.D. Fraia, L. Vanoli. Experimental and Numerical Investigation of Biosolid Gasification: Equilibrium-Based Modeling with Emphasis on the Effects of Different Pretreatment Methods. Industrial & Engineering Chemistry Research. 59 (2019) 299-307.
[35] Y. Cao, Q. Wang, J. Du, J. Chen. Oxygen-enriched air gasification of biomass materials for high-quality syngas production. Energy Conversion and Management. 199 (2019).
[36] R. Tavares, E. Monteiro, F. Tabet, A. Rouboa. Numerical investigation of optimum operating conditions for syngas and hydrogen production from biomass gasification using Aspen Plus. Renewable Energy. 146 (2020) 1309-14.
[37] Y. Yang, R.K. Liew, A.M. Tamothran, S.Y. Foong, P.N.Y. Yek, P.W. Chia, et al. Gasification of refuse-derived fuel from municipal solid waste for energy production: a review. Environ Chem Lett. (2021) 1-14.
[38] F. Wang, B. Cheng, Z.J. Ting, W. Dong, H. Zhou, E. Anthony, et al. Two-Stage Gasification of Sewage Sludge for Enhanced Hydrogen Production: Alkaline Pyrolysis Coupled with Catalytic Reforming Using Waste-Supported Ni Catalysts. ACS Sustainable Chemistry & Engineering. 8 (2020) 13377-86.
[39] A. AlNouss, G. McKay, T. Al-Ansari. A techno-economic-environmental study evaluating the potential of oxygen-steam biomass gasification for the generation of value-added products. Energy Conversion and Management. 196 (2019) 664-76.
[40] F. Emun, M. Gadalla, T. Majozi, D. Boer. Integrated gasification combined cycle (IGCC) process simulation and

optimization. Computers & Chemical Engineering. 34 (2010) 331-8.
[41] C. Madeddu, M. Errico, R. Baratti. CO2 Capture by Reactive Absorption-Stripping: Modeling, Analysis and Design. Springer2018.
[42] J. Park, S.Y. Lee, J. Kim, W. Um, I.-B. Lee, C. Yoo. Energy, safety, and absorption efficiency evaluation of a pilot-scale H2S abatement process using MDEA solution in a coke-oven gas. Journal of Environmental Chemical Engineering. 9 (2021).
[43] R.S. Cavaignac, N.L. Ferreira, R. Guardani. Techno-economic and environmental process evaluation of biogas upgrading via amine scrubbing. Renewable Energy. 171 (2021) 868-80.
[44] P.J. Robinson, W.L. Luyben. Integrated Gasification Combined Cycle Dynamic Model: H2S Absorption/Stripping, Water−Gas Shift Reactors, and CO2 Absorption/Stripping. Industrial & Engineering Chemistry Research. 49 (2010) 4766-81.
[45] Y. Su, L. Lü, W. Shen, S.a. Wei. An efficient technique for improving methanol yield using dual CO2 feeds and dry methane reforming. Frontiers of Chemical Science and Engineering. 14 (2019) 614-28.
[46] K.M.V. Bussche, G.F. Froment. A Steady-State Kinetic Model for Methanol Synthesis and the Water Gas Shift Reaction on a Commercial Cu/ZnO/Al2O3Catalyst. Journal of Catalysis. 161 (1996) 1-10.
[47] W.L. Luyben. Principles and case studies of simultaneous design. John Wiley & Sons2012.
[48] É.S. Van-Dal, C. Bouallou. Design and simulation of a methanol production plant from CO2 hydrogenation. Journal of Cleaner Production. 57 (2013) 38-45.
[49] X. Zhao, F. You. Waste respirator processing system for public health protection and climate change mitigation under COVID-19 pandemic: Novel process design and energy, environmental, and techno-economic perspectives. Appl Energy. 283 (2021) 116129.
[50] H. Kim, P. B Parajuli, F. Yu, E. P Columbus. Economic Analysis and Assessment of Syngas Production using a Modeling Approach. 2011 Louisville, Kentucky, August 7-10, 2011. ASABE, St. Joseph, MI, 2011.
[51] C. Maxwell. Cost Indices. 2021, Avaliable: https://wwwtoweringskillscom/financial-analysis/cost-indices/#chemical-engineering-plant-cost-index-cepci.
[52] Sludge transportation fees. 2021, Avaliable: https://wwwgdjlwlcom/wuliu_281044.
[53] G. Towler, R. Sinnott. Chemical engineering design: principles, practice and economics of plant and process design. Butterworth-Heinemann2021.
[54] D. Xiang, S. Yang, X. Li, Y. Qian. Life cycle assessment of energy consumption and GHG emissions of olefins production from alternative resources in China. Energy Conversion and Management. 90 (2015) 12-20.
[55] H. Xu, X. Wang, Y. Zou, L. Wang. Exergy, economic and environmental assessment of sec-butyl acetate hydrolysis to sec-butyl alcohol using a combined reaction and extractive distillation system. Fuel. 286 (2021) 119372.
[56] G. Li, Z. Liu, F. Liu, B. Yang, S. Ma, Y. Weng, et al. Advanced exergy analysis of ash agglomerating fluidized bed gasification. Energy Conversion and Management. 199 (2019).
[57] T.J. Kotas. The exergy method of thermal plant analysis. Elsevier2013.
[58] M. Atienza-Martínez, J. Ábrego, J.F. Mastral, J. Ceamanos, G. Gea. Energy and exergy analyses of sewage sludge thermochemical treatment. Energy. 144 (2018) 723-35.
[59] J.M. de Andrés, A. Narros, M.E. Rodríguez. Air-steam gasification of sewage sludge in a bubbling bed reactor: Effect of alumina as a primary catalyst. Fuel Processing Technology. 92 (2011) 433-40.
[60] M. La Villetta, M. Costa, N. Massarotti. Modelling approaches to biomass gasification: A review with emphasis on the stoichiometric method. Renewable and Sustainable Energy Reviews. 74 (2017) 71-88.
[61] P. Nikolaidis, A. Poullikkas. A comparative overview of hydrogen production processes. Renewable and Sustainable Energy Reviews. 67 (2017) 597-611.
[62] H. Wang, Y. Su, D. Wang, S. Jin, S.a. Wei, W. Shen. Optimal Design and Energy-Saving Investigation of the Triple

CO2 Feeds for Methanol Production System by Combining Steam and Dry Methane Reforming. Industrial & Engineering Chemistry Research. 59 (2020) 1596-606.
[63] Polaris water treatment, How much is the sludge treatment subsidy per ton? 2021, Avaliable: https://huanbaobjxcomcn/news/20210729/1166581shtml.
[64] IRENA AND METHANOL INSTITUTE (2021), Innovation Outlook : Renewable Methanol, International Renewable Energy Agency, Abu Dhabi.
[65] CEIC DATA, Hong Kong SAR, China Bank Lending Rate. 2022, Avaliable: https://wwwceicdatacom/en/indicator/hong-kong/bank-lending-rate.
[66] K.J. Ptasinski, C. Hamelinck, P.J.A.M. Kerkhof. Exergy analysis of methanol from the sewage sludge process. Energy Conversion and Management. 43 (2002) 1445-57.